NATURAL VIBRATIONS OF A STEEL-CONCRETE CYLINDRICAL SHELL IN A SOIL MEDIUM

Andrei Dmitriev*, Vladimir Sokolov, Tatyana Maltseva

Industrial University of Tyumen, 38 Volodarskogo St., Tyumen, Russia

*Corresponding author's email: dmitrievav@tyuiu.ru

Abstract

Introduction. Cylindrical shells embedded in the soil medium are generally used in pipeline transportation. To prevent damage to pipelines by concrete weights when the structure surfaces in a waterlogged environment, it is proposed to use concrete pipe products, with the inner part made of steel and the outer part formed by a concrete layer 30-50 mm thick. In this case, the designer faces the question of which calculation method to use for determining the natural vibration frequencies. Purpose of the study: To compare the values of natural vibration frequencies of a large-diameter steelconcrete gas pipeline in the ground, obtained using an analytical dependency, with the values determined in the Lira software package. Methods: The first method of determining frequency is based on an analytical expression obtained using the semi-momentless theory of cylindrical shells. The second method is based on the finite element method with the construction of a computational model in the Lira-SAPR software. Modeling of steel and concrete layers of the composite shell in the software package was carried out using 4-node plates, which are combined into a common structure with the help of perfectly rigid bodies (PRB). In the first case, the calculation for the soil medium surrounding the shell was carried out by creating a mass (measuring 5.3×5.3 meters) using volumetric bodies, while in the second case, it was done by setting a coefficient of subgrade reaction for the concrete layer. Results: We established that the second method of setting soil conditions allows a 5-6 times reduction in data entry time while achieving the same results. The discrepancy in the natural vibration frequencies for the research object, determined by the analytical method and the finite element method (FEM), does not exceed 10 %, and for the first three frequencies of the spectrum, it is no more than 6 %. Therefore, all methods are applicable. However, the use of an analytical expression allows calculations to be performed 10 times faster and does not require specialized software, making it more advantageous in the design based on frequency characteristics.

Keywords: natural vibrations; finite element method; semi-momentless theory of cylindrical shells; frequency.

Introduction

Cylindrical shells laid in a soil medium are generally used in the oil and gas industry for the transportation of hydrocarbons. The main pipeline is a multi-kilometer structure that is laid in various soil conditions, including areas with anticipated waterlogging and in waterlogged soils. Balancing of such sections is carried out using encircling concrete weights, which can damage the original geometry of the pipe section during maintenance or operation, thereby negatively affecting the reliability of the structure. One of the options to prevent such scenarios is the use of concrete pipe products, where the inner part is made of large-diameter steel pipes (d<1000 mm) with a parameter of $0.015 \le h/R \le 0.05$, and the outer part is formed by a concrete layer 30-50 mm thick. The reliability of such structures must be ensured by proper calculations during the design phase, one of the tasks of which is to ensure vibration resistance. In this case, the designer faces the question of which calculation method to use to determine the frequencies and modes of natural vibrations when constructing the pipeline based on frequency characteristics.

In the analyzed open sources published over the last 10 years, an approach using analytical expressions is proposed, as well as the application of the semi-analytical finite element method (FEM) in various software packages. For example, in the works of Shao et al. (2022), Shui et al. (2023), and Tan and Tang (2023), it is proposed to use analytical dependencies, which were obtained for a calculation scheme in the form of a rod, to determine the natural vibration frequencies of single-layer pipelines, taking into account the flow velocity of the fluid. This approach does not account for the deformation of the section and can be used for thick-walled cylindrical shells with parameters 0.07 < h/R < 0.125. Vibrational processes for cylindrical shells partially supported on the ground, based on the rod theory, were investigated by Xü et al. (2018). Leontiev and Travush (2020) studied the vibrations of an underwater pipeline for the pipe-fluid-soil system; however, the paper does not cover the issue of internal working pressure, which prevents the deformation of the cylindrical shell in the radial direction and is undoubtedly present during the transportation of oil or gas products. Shakiryanov and Akhmedyanov (2020) as well as

Yulmukhametov et al. (2020) studied the influence of internal non-stationary pressure on bending vibrations for computational models of closed cylindrical shells, but did not address the issue of the external environment surrounding the shell. Farshidianfar and Oliazadeh (2012), Lee and Kwak (2015), Oliazadeh et al. (2013) used various shell theories to determine the natural frequencies of pipeline vibrations: Soedel, Flügge, Morley-Koiter, and Donnell. The result of the solution using these theories is a determinant, which, when extended, calculates the frequency of natural vibrations. The work by Piacsek and Harris (2019) is analogous, but with the focus on aluminum structures. In (Kumar et al., 2015) and (Kumar et al., 2017), radial oscillations are studied without considering soil conditions, and the solution is obtained using the semimomentless theory of cylindrical shells by Vlasov-Novozhilov. In (Sokolov and Razov, 2020), analytical dependencies were obtained for determining the natural vibration frequencies of semi-underground large-diameter pipelines. In (Bochkarev, 2022), a similar approach was implemented for a twoparameter foundation, but without considering the effect of longitudinal compressive force and internal pressure. Shahbaztabar et al. (2019) examined the natural frequencies of a metal-ceramic cylindrical shell embedded in a Pasternak elastic foundation, but did not consider internal pressure. The works by Alshabatat and Zannon (2021), Baghlani et al. (2020), and Ebrahimi (2022) were dedicated to three-layer shells. However, the functionality of the solutions obtained is extremely limited, as they do not take into account the internal pressure on the shell wall, the longitudinal compressive force, or the resistance of the medium that prevents wall deformation. Jain et al. (2016) used a software based on the finite element method and developed a methodology for modeling and determining the natural vibration frequencies for a cylindrical shell in ANSYS with various types of constraints, but without considering the external environment, and compared the values with the previously obtained results. Kumar et al. (2015) used ABAQUS to model and determine the frequency spectrum, while Dyachenko et al. (2019) used the ANSYS software; subsequently, the authors compared the obtained results with the results of calculations using analytical formulas. Dashevskij et al. (2021) obtained the natural frequencies for a metro tunnel using MSC Patran/Nastran software, but without using analytical dependencies. The literature review shows that numerous works are dedicated to this topic, and the approaches to solving the problem are diverse.

The aim of this work is to analyze the influence of soil conditions on the values of the natural vibration frequencies for a steel-concrete pipeline, as well as to compare the obtained results for the two proposed

methods for determining frequencies to identify the optimal approach to solving the problem.

Subject, objectives, and methods

The object of the study is a section of a cylindrical two-layer shell designed for the transportation of natural gas, with a radius of the main steel layer R=0.71 m and a thickness of $h_2=18$ mm. The thickness of the second concrete layer is $h_1=40$ mm. The length of the considered section of the cylindrical shell is taken as 7, 8, and 9 m. The moduli of elasticity for concrete and steel, as well as the density of the layers, are respectively equal to $E_1=3.24711\cdot10^{10}$ (N/m²), $E_2=2.06\cdot10^{11}$ (N/m²), $V_1=24.516.6$ (N/m³), $V_2=76.982.2$ (N/m³). The Poisson's ratio for steel and concrete of class B30 is assumed to be V=0.3. The internal pressure is assumed to be $P_0=0$ MPa, and the longitudinal compressive force is also not considered.

The problem considers four types of soil conditions:

- In the first case, the structure is placed in a peat mass with the following parameters: soil density $\gamma_{gr} = 11,770 \text{ N/m}^3$; soil modulus of elasticity $E_{qr} = 500,000 \text{ N/m}^2$; soil Poisson's ratio $v_{qr} = 0.49$.
- In the second case, the soil medium is represented by uncompacted fill soil with the following parameters: soil density $\gamma_{gr} = 16,660 \text{ N/m}^3$; soil modulus of elasticity $E_{gr} = 3,000,000 \text{ N/m}^2$; soil Poisson's ratio $v_{qr} = 0.35$.
- The third case considers compacted fill soil with the following parameters: soil density $\gamma_{gr} = 17,660 \text{ N/m}^3$; soil modulus of elasticity $E_{gr} = 5,000,000 \text{ N/m}^2$; soil Poisson's ratio $v_{cr} = 0.35$.
- Poisson's ratio $v_{gr} = 0.35$.

 The fourth case is clay: soil density $\gamma_{gr} = 19,620 \text{ N/m}^3$; soil elasticity modulus $E_{gr} = 20,000,000 \text{ N/m}^2$; soil Poisson's ratio $v_{gr} = 0.42$.

The *first method* for determining the natural frequency is based on the use of an analytical expression derived for the calculation scheme shown in Fig. 1.

We consider a section of a steel gas pipeline in a concrete casing, with the ends of the section assumed to be hinged. The pipeline is buried in the ground no more than half its diameter from the top generatrix to the ground level. In the governing equation for this situation, in addition to the internal pressure p_0 in the cylindrical shell, the elastic resistance of the soil medium $q_{\rm gr}$ is taken into account, while the active soil pressure on the wall of the cylindrical shell is not considered, as it is minimal. The added mass of the soil, which may be involved in the vibration, and the longitudinal compressive force that appears during thermal deformations or uneven settlement of the structure, are also not taken into account.

The resistance of the soil medium is assumed to be radial and is described by expression (1), which corresponds to the distribution pattern along the circumference of the shell as shown in Fig. 1:

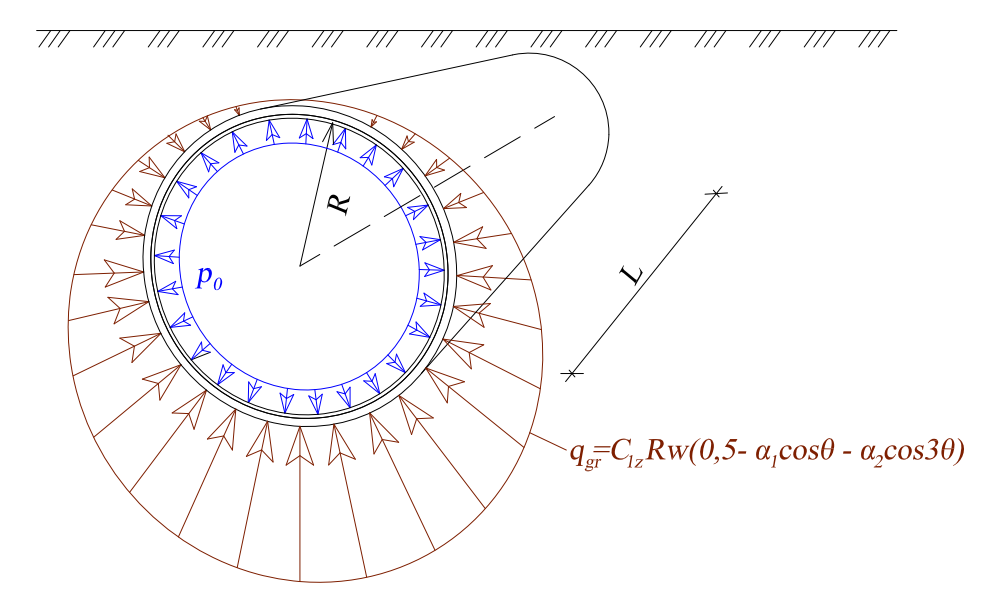


Fig. 1. Calculation scheme

 $q_{gr}=C_{1z}Rwig(0,5-lpha_1\cos\theta-lpha_2\cos3\thetaig),$ (1) here: q_{gr} — elastic resistance of the soil medium, preventing deformation of the cross-section; C_{1z} —coefficient of subgrade reaction; R—radius of the shell; w—displacement in the radial direction; α_1 and α_2 —coefficients ranging from 0.25 to 0.75, which are determined by selection depending on the radius of the cylindrical shell.

In solving the given problem, we applied the semi-momentless theory of cylindrical shells by Vlasov–Novozhilov, based on which the equilibrium equations for the cylindrical shell are written as follows:

$$\begin{split} \frac{\partial T_1}{\partial \xi} + \frac{\partial S}{\partial \theta} + R Q_2 \tau &= -R X_1, \\ \frac{\partial T_2}{\partial \theta} + \frac{\partial S}{\partial \xi} + \frac{R}{R_2^*} Q_2 &= -R X_2, \\ \frac{\partial Q_2}{\partial \theta} - \frac{R}{R_2^*} T_2 - \frac{R}{R_1^*} T_1 &= -R X_3, \\ \frac{\partial M_1}{\partial \xi} + \frac{\partial H}{\partial \theta} - R Q_1 &= 0, \quad \frac{\partial M_2}{\partial \theta} - \frac{\partial H}{\partial \xi} - R Q_2 &= 0. \end{split} \tag{2}$$

Transforming expressions (2) taking into account the relations of the semi-momentless theory (3):

$$\left(\frac{\partial \mathbf{v}}{\partial \theta} + \mathbf{w} = 0; \frac{\partial \mathbf{v}}{\partial \xi} + \frac{\partial \mathbf{u}}{\partial \theta} = 0; \vartheta_2 = \frac{\partial \mathbf{w}}{\partial \theta} - \mathbf{v}\right), \quad (3)$$

we obtain the equation in forces (4)

$$\begin{split} \frac{\partial^{2} T_{1}}{\partial \xi^{2}} + \frac{\partial}{\partial \xi} \left(\tau \frac{\partial M_{2}}{\partial \theta} \right) - \frac{1}{R^{2}} \cdot \frac{\partial^{3}}{\partial \theta^{3}} \left(R_{2}^{*} \frac{\partial M_{2}}{\partial \theta} \right) - \\ - \frac{\partial}{\partial \theta} \left(\frac{1}{R_{2}^{*}} \frac{\partial M_{2}}{\partial \theta} \right) + \frac{\partial^{2}}{\partial \theta^{2}} \left(\frac{R_{2}^{*}}{R_{1}^{*}} T_{1} \right) + \\ + R \frac{\partial X_{1}}{\partial \xi} - R \frac{\partial X_{2}}{\partial \theta} - \frac{\partial^{2}}{\partial \theta^{2}} \left(R_{2}^{*} X_{3} \right) = 0. \end{split} \tag{4}$$

Inertial components $X_1 = -Rh\rho_0 \frac{\partial^2 u}{\partial t^2}$ in the longitudinal direction, $X_2 = -Rh\rho_0 \frac{\partial^2 v}{\partial t^2}$ in the circumferential direction, as well as

$$X_3 = -R h \rho_0 \frac{\partial^2 w}{\partial t^2} + p_0 -$$

$$-C_{1z} R w (0, 5 - \alpha_1 \cos \theta - \alpha_2 \cos 3\theta),$$

in the radial direction are substituted into (4) and considering the dependencies between forces and deformations, displacements and deformations, without taking into account the nonlinear components (due to their insignificance compared to the linear ones), we obtain the linearized differential equation of motion in displacements:

$$\frac{\partial^{3} u}{\partial \xi^{3}} + \eta h_{v}^{2} \frac{\partial^{3}}{\partial \theta^{3}} \left(\frac{\partial^{2} 9_{2}}{\partial \theta^{2}} + 9_{2} \right) + \\
+ 2 \frac{\partial^{2}}{\partial \theta^{2}} \left(\frac{\partial^{2} w}{\partial \xi^{2}} \varepsilon_{0} \right) - \frac{R}{E_{0} h} p_{0} \frac{\partial^{3} 9_{2}}{\partial \theta^{3}} + \frac{1}{2} \frac{R^{2} C_{1z}}{E_{0} h} \frac{\partial^{2} w}{\partial \theta^{2}} - \\
- \frac{R^{2} \rho_{0}}{E h} \left(\frac{\partial^{3} u}{\partial \xi \partial t^{2}} - \frac{\partial^{3} v}{\partial \xi \partial t^{2}} - \frac{\partial^{3} w}{\partial \theta^{2} \partial t} \right) - \\
- \frac{R^{2} \alpha_{1} C_{1z}}{E_{0} h} \left(\frac{\partial^{2} w}{\partial \theta^{2}} \cos \theta - 2 \frac{\partial w}{\partial \theta} \sin \theta - w \cos \theta \right) - \\
- \frac{R^{2} \alpha_{2} C_{1z}}{E_{0} h} \left(\frac{\partial^{2} w}{\partial \theta^{2}} \cos 3\theta - \frac{\partial w}{\partial \theta} 6 \sin 3\theta - 9w \cos 3\theta \right) = 0. (5)$$

This expression contains unknown displacements in the longitudinal u, circumferential v, and radial w directions, as well as the angle of rotation of the initial and deformed states ϑ_2 . By incorporating the semi-momentless theory relations (3), we obtain a complete system of differential equations.

The hinged support of the shell ends is described by expressions (6):

$$v\left\{\xi = 0, \xi = \frac{L}{R} = 0\right\}, \ \theta_2\left\{\xi = 0, \xi = \frac{L}{R} = 0\right\};$$

$$w\left\{\xi = 0, \xi = \frac{L}{R} = 0\right\}; \ \frac{\partial^2 w}{\partial \xi^2} \left\{\xi = 0, \xi = \frac{L}{R} = 0\right\}.$$
 (6)

The solution is then carried out using the method of separation of variables. The double row for relative radial displacement w is written as (7):

$$w = \sum_{m} \sum_{n} b_{mn} \ \varphi(t) \sin(\lambda_n \xi) \cos(m\theta). \tag{7}$$

We determine displacements u, v, as well as ϑ from (7) taking into account (3); they are described by expressions (8):

$$u = \sum_{m} \sum_{n} b_{mn} \frac{\lambda_{n}}{m^{2}} \varphi(t) \cos(\lambda_{n} \xi) \cos(m\theta);$$

$$v = \sum_{m} \sum_{n} b_{mn} \frac{1}{m} \varphi(t) \sin(\lambda_{n} \xi) \sin(m\theta);$$

$$\theta_{2} = -\sum_{m} \sum_{n} b_{mn} \frac{m^{2} - 1}{m} \varphi(t) \sin(\lambda_{n} \xi) \sin(m\theta). \quad (8)$$

The vibration process for a cylindrical shell, occurring according to the harmonic law, is represented by the function $\varphi(t)$ in the form:

$$\varphi(t) = \sin \omega_{mn} t; \ \varphi''(t) = -\omega^2 \sin \omega_{mn} t, \tag{9}$$

where ω_{mn} is the natural frequency of vibrations.

By substituting expressions (7) and (8) into (5) taking into account (9), performing transformation, and denoting the coefficients of the unknowns as a_{ii} , we obtain system (10):

Let us represent system (10) in the form of expression (11):

$$a_{m,m-3}b_{m-3,n} + a_{m,m-1}b_{m-1,n} + a_{m,m}b_{m,n} + a_{m,m+1}b_{m+1,n} + a_{m,m+3}b_{m+3,n} = 0,$$
(11)

for which the a_{ij} coefficients are determined by expressions (12):

$$a_{m,m} = A_{n,m} - B_{n,m} \omega_{nm}^{2}; \ a_{m,m\pm 1} = -\frac{m^{2} (m\pm 1)^{2}}{2} q_{gr}^{*} \alpha_{1};$$

$$a_{m,m\pm 3} = -\frac{m^{2} [(m\pm 3)^{2} - 1]}{2} q_{gr}^{*} \alpha_{2};$$

$$A_{n,m} = \lambda_{n}^{4} + \eta m^{4} (m^{2} - 1)(m^{2} - 1 + \frac{p^{*}}{\eta}) + C^{*} m^{4} - \lambda_{n}^{4} m^{4} P / n^{2};$$

$$B_{n,m} = \rho^{*} Rh(\lambda^{2} h_{v} + m^{2} + m^{4}). \tag{12}$$

Expression (11) is solved using the matrix method, the result of which is presented in the form of (13):

$$\begin{vmatrix} d_{11} - \lambda & d_{12} & d_{13} & d_{14} & \dots & d_{1n} \\ d_{21} & d_{22} - \lambda & d_{23} & d_{24} & \dots & d_{2n} \\ d_{31} & d_{32} & d_{33} - \lambda & d_{34} & \dots & d_{3n} \\ d_{41} & d_{42} & d_{43} & d_{44} - \lambda & \dots & d_{4n} \\ \dots & \dots & \dots & \dots & \dots & \dots \\ d_{p-41} & d_{p-31} & d_{p-21} & d_{p-11} & \dots & d_{pn} - \lambda \end{vmatrix} = 0, \quad (13)$$

$$d_{m,m} = \frac{0_{m,m}}{B_{n,m}}; \ d_{m,m\pm 1} = \frac{a_{m,m\pm 1}}{B_{n,m}}; \ d_{m,m\pm 2} = \frac{a_{m,m\pm 3}}{B_{n,m}},$$

and the coefficients $A_{n,m}, B_{n,m}, a_{m,m+1}, a_{m,m+3}$ are found using (12).

Subsequently, by expanding the determinant, we find the eigenvalues λ , where $\lambda = \omega_{n,m}^2$ is the square of the circular frequency of natural vibrations (1/s2) for the cylindrical shell.

Having analyzed the actions of the side coefficients of determinant (13), we established that their influence on the final result is no more than 2 %. Therefore, we will consider them equal to zero in the future, and determinant (13) takes the form:

$$\begin{vmatrix} d_{11} - \lambda & 0 & 0 & 0 & \dots & 0 \\ 0 & d_{22} - \lambda & 0 & 0 & \dots & 0 \\ 0 & 0 & d_{33} - \lambda & 0 & \dots & 0 \\ 0 & 0 & 0 & d_{44} - \lambda & \dots & 0 \\ \dots & \dots & \dots & \dots & \dots & \dots \\ 0 & 0 & 0 & 0 & \dots & d_{pn} - \lambda \end{vmatrix} = 0. (14)$$

By solving the determinant (14), we obtain expressions for determining the frequencies of natural vibrations for pipelines:

$$\omega_{nm} = \frac{1}{2\pi} \sqrt{\frac{\lambda_n^4 + \eta \cdot m^4 \left(m^2 - 1\right) \left(m^2 - 1 + \frac{p^*}{\eta}\right) + C_{1z}^* \cdot m^4}{\rho_{sh}^* \cdot R_0 \cdot h\left(\lambda_n^4 h_{\mathbf{v}} + m^4 + m^2\right)}}, (15)$$

here:

n is the number of half-waves in the longitudinal direction;

m is the number of half-waves in the circumferential

 $\lambda_n = n\pi R_0 / L\sqrt{h_v}$ is the length parameter of a two-layer cylindrical shell;

L is the length of the section (m);

 $R_0 = R - Z_0$ is the reduced shell radius (m);

$$R_0 = R_1 + E_0$$
 is the reduced shell radius (in),
 R is the radius of the steel layer of the shell (m);
 $Z_0 = \frac{E_1 h_1^2 - E_2 h_2^2}{2(E_1 h_1 + E_2 h_2)}$ is the distance from the

connection layer to the original surface (m) (Fig. 2);

 $h_{\rm a}$ is the thickness of the concrete layer of the shell (m):

 h_2 is the thickness of the steel layer of the shell

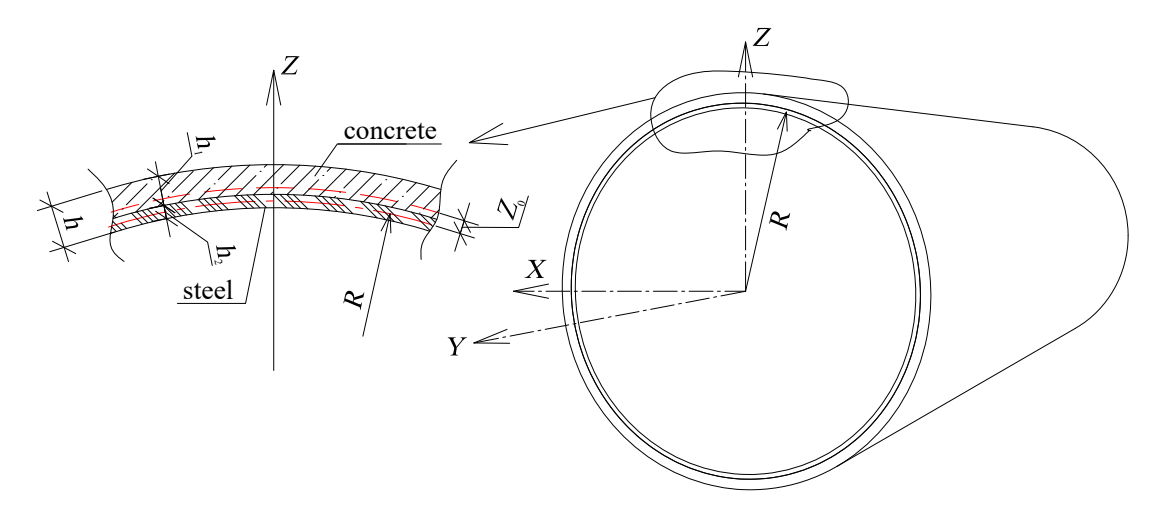


Fig. 2. Geometric dimensions of a two-layer shell

 $h = h_1 + h_2$ is the wall thickness of the two-layer shell (m);

 E_1 is the modulus of elasticity of the concrete layer (N/m²);

 E_2 is the modulus of elasticity of the steel layer (N/m²);

 $h_{\rm v} = h/R_0\sqrt{12(1-{\rm v}^2)}$ is the parameter of the relative thickness of the shell;

v is Poisson's ratio:

 $\eta = E_v / E_0$ is inhomogeneity coefficient;

 $E_{\rm v} = \left(1 - {\rm v}^2\right) \cdot 12D/\,h^3 \quad {\rm is} \quad {\rm reduced} \quad {\rm modulus} \quad {\rm of} \quad {\rm elasticity} \; ({\rm bending});$

$$D = \frac{1}{3(1-v^2)} \times$$

$$\times \left[E_1 \left\{ \left(h_1 - Z_0 \right)^3 + Z_0^3 \right\} + E_2 \left\{ \left(h_2 + Z_0 \right)^3 - Z_0^3 \right\} \right]$$

is reduced bending stiffness;

 $E_0 = \left[E_1 h_1 + E_2 h_2 \right] / h$ is reduced modulus of elasticity (tension/compression);

 $p^* = p_0 \left(R_0 / E_0 h \cdot h_v^2 \right)$ is internal working pressure parameter;

 ho_0 is internal pressure in a two-layer shell (N/m²); $ho_{sh}^* =
ho_0 \left(R_0 / E_0 \cdot h \cdot h_v^2 \right)$ is the parameter of the material density of the shell (s²/m²);

 $\rho_0 = \frac{1}{g} \Big[\big(\gamma_1 h_1 + \gamma_2 h_2 \big) / h \Big] \text{ is the reduced specific}$ weight of the shell material (N·s²/m³);

 γ_1 is density of concrete (N/m³);

 γ_1 is density of steel (N/m³);

 $C_{1z}^* = R_0^2 C_{1z} / E_{gr} h \cdot h_v^2$ is the reduced coefficient of subgrade reaction;

 $C_{1z} = E_{gr} / R_0 \left(1 + v_{gr} \right)$ is the coefficient of subgrade reaction for a cylindrical shell (N/m³);

 $E_{\rm or}$ is modulus of elasticity for soil (N/m²).

To calculate the natural frequencies of vibrations using the *second method*, we used the Lira-SAPR software. The modeling of each layer of the two-layer shell (Fig. 3) was carried out using four-node plate elements (Type 41) with dimensions of 0.1×0.1 m. Their geometric position corresponded to the position of the element of the midsurface for each layer. The stiffness characteristics of the layers are shown in Fig. 4. To ensure the synergy of the layers, we used displacement combinations for each corresponding node by setting perfectly rigid bodies (PRB). To fasten the shell ends according to the hinged-fixed scheme, we introduced a restriction on the linear displacements of the boundary nodes along the *Z* and *Y* axes.

Modeling of the medium (soil) in which the shell is placed was carried out in two ways:

- In the first method, we created a mass of universal spatial eight-node isoparametric finite elements (Type 36) with dimensions of 0.1×0.1×0.1 m. The overall size of the created medium mass in cross-section is 5.3×5.3 m. The stiffness characteristics of the volumetric elements of the soil mass are shown in Fig. 5.
- There was no soil mass created in the second method, and the elastic resistance of the soil was accounted for by assigning a coefficient of subgrade reaction (Fig. 6) for the plate concrete elements $C_{1z}=473,620~(\mathrm{N/m^3})$ for the first case of soil conditions, $C_{1z}=3,136,416~(\mathrm{N/m^3})$ for the second, $C_{1z}=5,227,360~(\mathrm{N/m^3})$ for the third, and $C_{1z}=19,878,694~(\mathrm{N/m^3})$ for the fourth.

Only the self-weight of the shell layers was considered as external loads (excluding the weight of the soil medium).

We determined natural vibration frequencies using "Modal Analysis", which forms the mass matrix of the structure, and the number of natural vibration modes, which in this case was set to ten. The mass matrix is formed based on the density of the elements (Fig. 7).

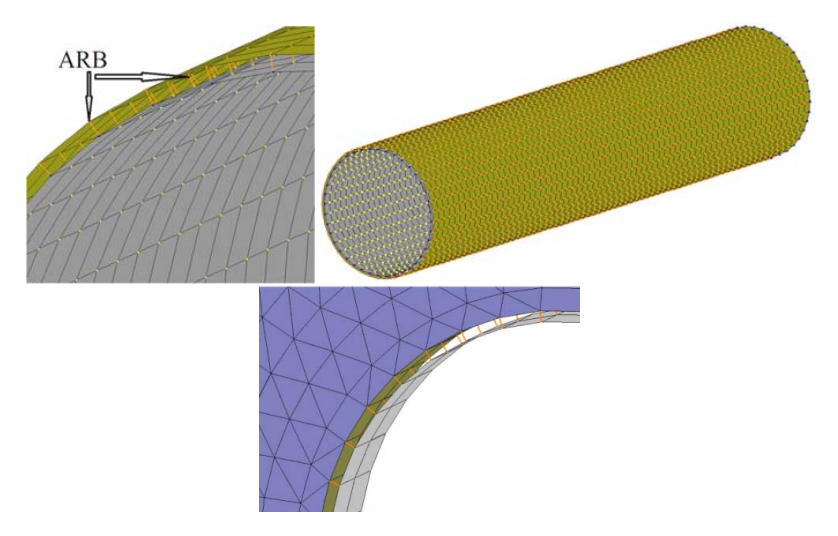


Fig. 3. Modeling of a composite cylindrical shell

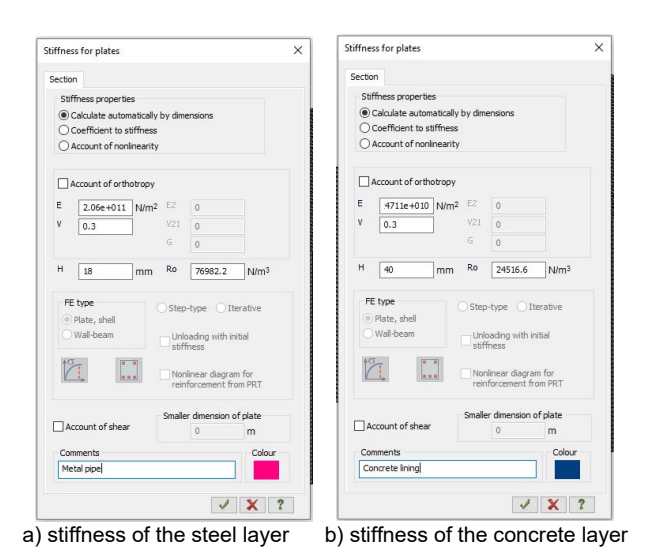


Fig. 4. Stiffness of plate elements of a composite shell

Results and discussion

All calculated natural vibration frequencies for different section lengths, as well as in various soil conditions, are compiled in Table for the ease of analysis. The first column presents the results of the calculation using expression (15); the second column contains the results of the calculation in the Lira software package with the set soil medium mass; the third one shows the results for the FEM with the set coefficient of subgrade reaction C_{1z} . The results correspond to seven vibration modes, images of which are shown in Fig. 8. For clarity, Fig. 9 shows the first three modes of vibration in the soil mass.

Analysis of the data in Table shows:

• For the considered section with a length of 7 m, the minimum frequencies are realized for ω_{12} , that is, with the flattening of the cross-section, and correspond to shell vibration modes, while for sections with lengths of 8 and 9 m, the minimum frequencies correspond to the ω_{11} mode (rod, without

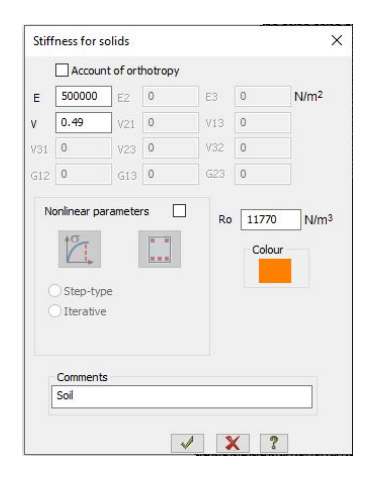


Fig. 5. Soil stiffness

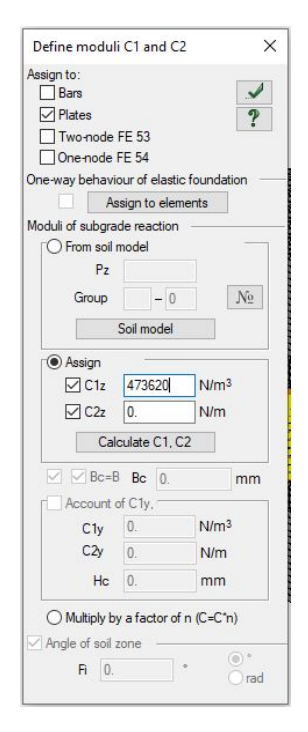


Fig. 6. Coefficient of subgrade reaction of the concrete layer

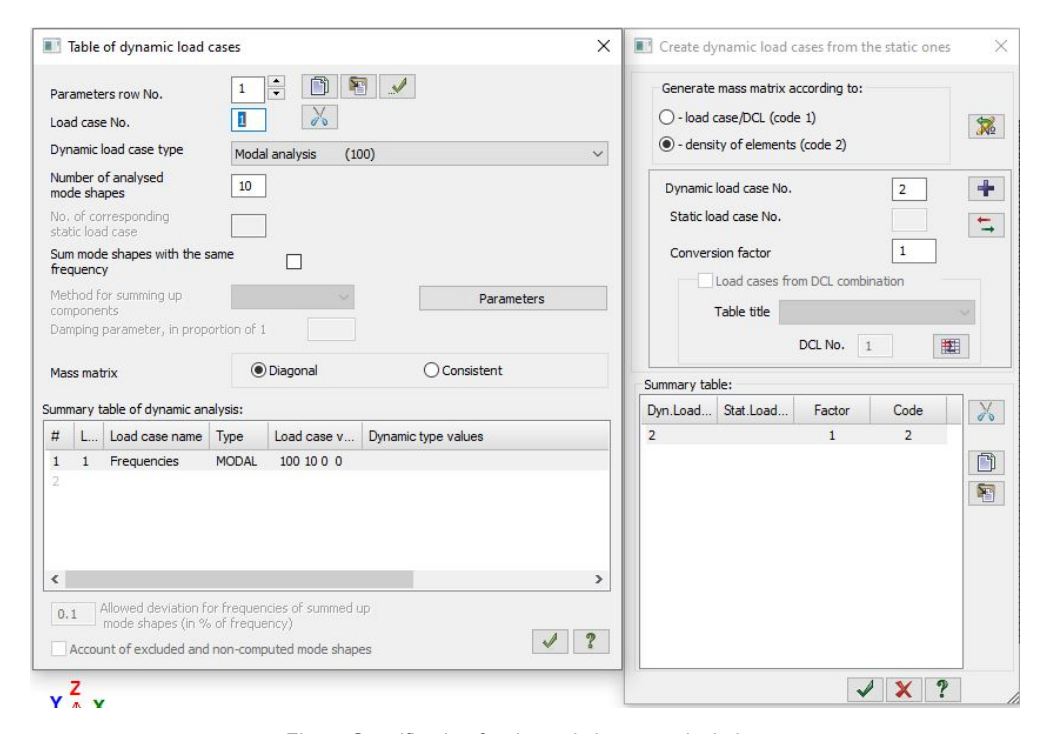


Fig. 7. Specification for dynamic impact calculation

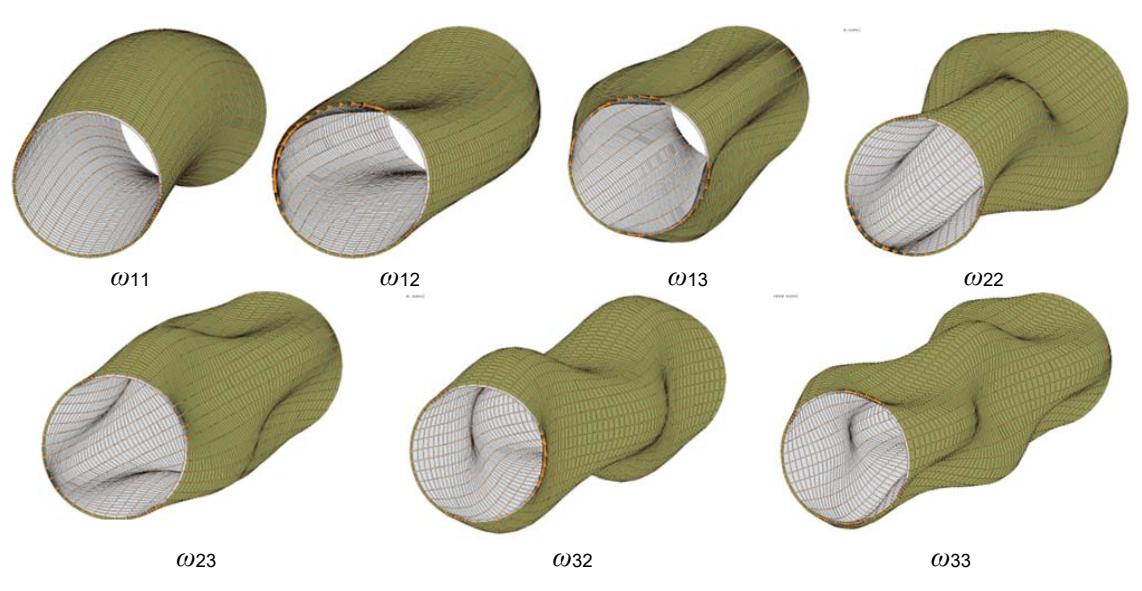


Fig. 8. Vibration modes for the considered section of the pipeline

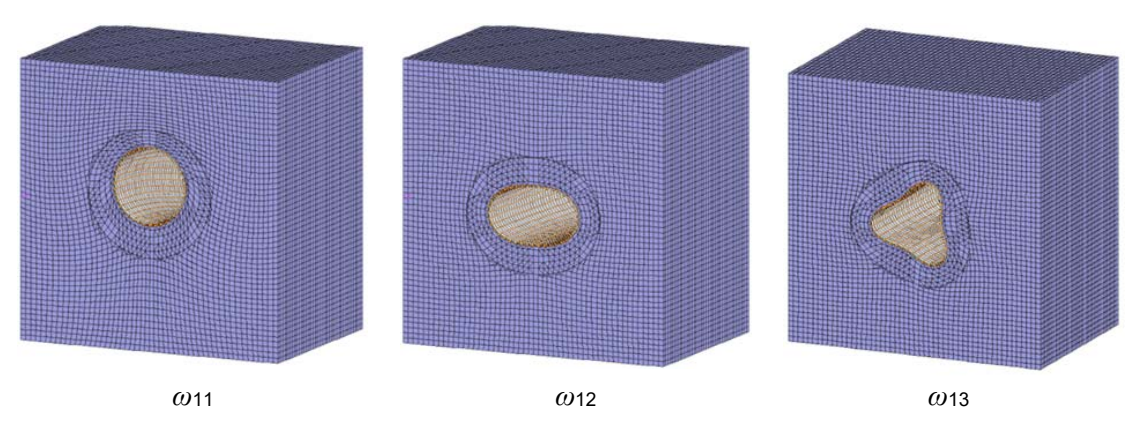


Fig. 9. Vibration modes for the considered section of the pipeline at n=1 in the soil mass (the mass size is 5.3×5.3 m in cross-section)

Results of determining the natural vibration frequencies by various methods for different soil conditions

Analytical formula (Hz)	Lira-SAPR mass (Hz)	Lira-SAPR coefficient of subgrade reaction C _{1z} (Hz)	Analytical formula (Hz)	Lira-SAPR mass (Hz)	Lira-SAPR coefficient of subgrade reaction C _{1z} (Hz)	Analytical formula (Hz)	Lira-SAPR mass (Hz)	Lira-SAPR coefficient of subgrade reaction C ₁₂ (Hz)	
1	2	3	1	2	3	1	2	3	
L=7 m (R/L=1/10)			L=8 m (R/L=1/11)			L=9 m (R/L=1/13)			
Peat $C_{1z} = 473,620 \text{ (N/m}^3), \gamma_{gr} = 11,770 \text{ N/m}^3; E_{gr} = 5 \cdot 10^5 \text{ N/m}^2; v_{gr} = 0.49.$									
ω ₁₁ =71.52	ω ₁₁ =69.80	ω ₁₁ =68.99	ω ₁₁ =55.16	ω ₁₁ =57.08	ω ₁₁ =56.04	ω ₁₁ =43.86	ω ₁₁ =48.4	ω ₁₁ =47.14	
$\omega_{12} = 64.23$	$\omega_{12} = 69.90$	ω ₁₂ =63.13	ω ₁₂ =62.53	ω ₁₂ =68.21	ω_{12} =67.58	ω ₁₂ =61.61	ω ₁₂ =67.2	ω ₁₂ =66.54	
ω ₁₃ =169.4	$\omega_{13} = 164.7$	ω ₁₃ =164.4	$\omega_{13} = 169.3$	ω ₁₃ =164.10	ω ₁₃ =163.8	ω ₁₃ =169.2	ω ₁₃ =163.8	ω ₁₃ =163.5	
ω ₂₂ =109.2	ω ₂₂ =109.6	ω ₂₂ =109.3	ω ₂₂ =92.18	ω ₂₂ =95.40	ω ₂₂ =95.01	ω ₂₂ =81.62	ω ₂₂ =86.2	ω ₂₂ =79.20	
$\omega_{23} = 174.3$	ω ₂₃ =174.6	ω ₂₃ =174.3	ω ₂₃ =172.1	ω ₂₃ =170.9	ω ₂₃ =170.6	ω ₂₃ =170.9	ω ₂₃ =168.7	ω ₂₃ = 168.4	
ω ₃₂ =211.9	ω ₃₂ =186.5	ω ₃₂ =186.3	ω ₃₂ =167.4	ω_{32} =154.8	ω_{32} =154.6	ω ₃₂ =137.6	ω_{32} =132.3	ω ₃₂ =132.0	
ω_{33} =194.6	ω ₃₃ =199.7	ω_{33} =199.5	ω ₃₃ =184.4	ω ₃₃ =188.2	$\omega_{33} = 187.9$	ω_{33} =178.7	ω_{33} = 181.3	$\omega_{33} = 180.7$	
Uncompacted fill soil $C_{1z} = 3,136,416 \text{ (N/m}^3), \gamma_{gr} = 16,660 \text{ N/m}^3; E_{gr} = 3\cdot10^6 \text{ N/m}^2; v_{gr} = 0.35.$									
ω ₁₁ =72.45	ω ₁₁ =70.57	ω ₁₁ =69.97	ω ₁₁ =56.37	ω ₁₁ =58.89	ω ₁₁ =57.25	ω ₁₁ =45.38	ω ₁₁ =50.49	ω ₁₁ =48.57	
ω ₁₂ =65.94	ω ₁₂ =71.61	ω ₁₂ =70.91	ω ₁₂ =64.29	ω ₁₂ =70.39	ω ₁₂ =69.26	ω ₁₂ =63.39	ω ₁₂ =69.39	ω ₁₂ =68.20	
ω ₁₃ =170.17	ω ₁₃ =166.13	ω ₁₃ =165.15	ω ₁₃ =170.05	ω ₁₃ =165.70	ω ₁₃ =164.62	ω ₁₃ =169.98	ω ₁₃ =165.36	ω ₁₃ =167.28	
ω ₂₂ =110.22	ω ₂₂ =110.79	ω ₂₂ =110.34	ω ₂₂ =93.37	ω ₂₂ =97.06	ω ₂₂ =96.17	ω ₂₂ =82.97	ω ₂₂ =88.03	ω ₂₂ =79.96	
ω ₂₃ =175.03	ω ₂₃ =175.98	ω ₂₃ =175.02	ω ₂₃ =172.87	ω ₂₃ =172.46	ω ₂₃ =171.16	ω ₂₃ =171.72	ω ₂₃ =170.25	ω ₂₃ =169.18	
ω ₃₂ =212.39	ω_{32} =187.30	ω ₃₂ =187.01	ω ₃₂ =168.07	ω ₃₂ =155.92	ω ₃₂ =155.31	ω_{32} =138.43	ω ₃₂ =133.54	ω ₃₂ =132.87	
ω ₃₃ =195.23	ω_{33} =200.98	ω ₃₃ =200.09	ω ₃₃ =185.07	ω_{33} =189.60	ω ₃₃ =188.58	ω ₃₃ =179.44	ω_{33} =182.46	ω ₃₃ =180.12	
Uncompacted fill soil $C_{1z} = 5,227,360 \text{ (N/m}^3), \gamma_{gr} = 17,660 \text{ N/m}^3; E_{gr} = 5.10^6 \text{ N/m}^2; \nu_{gr} = 0.35.$									
ω ₁₁ =73.17	ω ₁₁ =71.72	ω ₁₁ =70.72	ω ₁₁ =57.30	ω ₁₁ =60.85	ω ₁₁ =58.18	ω ₁₁ =46.53	ω ₁₁ =51.76	ω ₁₁ =49.68	
ω ₁₂ =67.26	ω ₁₂ =73.23	ω ₁₂ =72.12	ω ₁₂ =65.64	ω ₁₂ =72.38	ω ₁₂ =70.55	ω ₁₂ =64.76	ω ₁₂ =71.41	ω ₁₂ =69.56	
ω ₁₃ =170.75	ω ₁₃ =167.38	ω ₁₃ =165.77	ω ₁₃ =170.63	ω ₁₃ =167.02	ω ₁₃ =165.24	ω ₁₃ =170.57	ω ₁₃ =166.68	ω ₁₃ =164.89	
ω ₂₂ =110.99	ω ₂₂ =111.89	ω ₂₂ =110.13	ω ₂₂ =94.29	ω ₂₂ =98.54	ω ₂₂ =97.11	ω ₂₂ =84.01	ω ₂₂ =89.65	ω ₂₂ =88.12	
ω ₂₃ =175.59	ω ₂₃ =177.19	ω ₂₃ =175.61	ω_{23} =173.43	ω ₂₃ =173.76	ω ₂₃ =171.72	ω ₂₃ =172.29	ω ₂₃ =171.55	ω ₂₃ =170.17	
ω ₃₂ =212.79	ω_{32} =188.03	ω ₃₂ =187.38	ω_{32} =168.58	ω ₃₂ =156.88	ω ₃₂ =155.87	ω_{32} =139.05	ω_{32} =134.65	$\omega_{_{32}}$ =133.53	
ω ₃₃ =195.73	ω_{33} =202.09	ω ₃₃ =200.59	ω ₃₃ =185.59	ω ₃₃ =190.81	ω ₃₃ =189.12	$\omega_{_{33}}$ =179.98	$\omega_{_{33}}$ =183.69	ω ₃₃ =181.97	
Clay $C_{1z} = 19,878,694 \text{ (N/m}^3), \gamma_{gr} = 19,620 \text{ N/m}^3; E_{gr} = 2 \cdot 10^7 \text{ N/m}^2; v_{gr} = 0.42.$									
ω ₁₁ =78.01	ω ₁₁ =80.92	ω ₁₁ =75.81	ω ₁₁ =64.44	ω ₁₁ =77.37	ω ₁₁ =64.32	ω ₁₁ =53.97	ω ₁₁ =71.29	ω ₁₁ =56.79	
ω ₁₂ =75.82	ω ₁₂ =85.87	ω ₁₂ =80.09	ω ₁₂ =74.40	ω ₁₂ =88.80	ω ₁₂ =78.98	ω ₁₂ =73.64	ω ₁₂ =88.04	ω ₁₂ =78.11	
ω ₁₃ =174.76	ω ₁₃ =177.17	ω ₁₃ =170.14	ω ₁₃ =174.64	ω ₁₃ =177.59	ω ₁₃ =169.49	ω ₁₃ =174.58	ω ₁₃ =177.27	ω ₁₃ =169.16	
ω ₂₂ =116.31	ω ₂₂ =120.41	ω ₂₂ =116.59	ω ₂₂ =100.52	ω ₂₂ =110.79	ω ₂₂ =103.32	ω ₂₂ =90.96	ω ₂₂ =103.76	ω ₂₂ =94.94	
ω ₂₃ =179.48	ω ₂₃ =186.56	ω ₂₃ =179.59	ω_{23} =177.37	ω ₂₃ =183.98	ω ₂₃ =176.02	ω_{23} =176.26	ω ₂₃ =181.88	ω ₂₃ =174.27	
ω ₃₂ =215.54	ω ₃₂ =193.62	ω ₃₂ =190.64	ω ₃₂ =172.07	ω ₃₂ =164.79	ω ₃₂ =159.78	ω ₃₂ =143.30	ω_{32} =143.72	ω ₃₂ =138.08	
$\omega_{_{33}}$ =199.20	ω ₃₃ =209.42	ω ₃₃ =204.08	ω ₃₃ =189.27	ω ₃₃ =190.33	ω ₃₃ =192.81	ω ₃₃ =183.77	ω ₃₃ =193.46	ω ₃₃ =185.81	
Page of the control feature by the control fe			Personal flow and flo			Types I how may I have yet Section 1 S			
	$\omega_{_{11}}$		$\omega_{_{12}}$				$\omega_{_{13}}$		

cross-sectional deformation). All other vibration modes are shell-like.

- An increase in the length of the considered section by 1 m leads to a decrease in the value of the natural vibration frequencies by an average of 1.5–3.0 %, regardless of the method used to determine these values.
- An increase in the stiffness characteristics of the soil medium leads to higher values of the natural frequency of the steel-concrete-soil system. This is explained by the fact that the soil medium enhances the system's stiffness by preventing deformation of the cross-section.
- A comparison of the results for determining the natural vibration frequencies using expression (15) and software calculation shows that the difference for the first three frequencies does not exceed 6 %, and for the remaining results 10 %.
- The difference in the values of natural vibration frequencies determined using the finite element method with the specification of the soil mass (column 2) and by assigning the coefficient of subgrade reaction (column 3) does not exceed 2 %. Therefore, to reduce labor costs when creating the model, it is recommended to use the second method of modeling soil conditions. This method allows reducing the model loading time by five times and the data processing speed by the processor by at least ten times.

The results of the work done allow us to draw the following conclusions:

- The analytical method for determining frequencies using expression (15) has clear advantages over the finite element method, as it required 40 times less time to compute the data while yielding practically identical results.
- In the analytical method, the influence of internal working pressure can be accounted

for using parameter p. However, this factor is impossible to apply in the finite element method. When modeling this loading, the internal pressure is considered not as a force preventing the deformation of the cross-section, but as an additional mass that acts as a kind of damper, resulting in a sharp decrease in frequency values. Therefore, all the data in Table 1 were obtained at zero internal pressure.

Conclusions

- 1. The discrepancy in the natural vibration frequencies for the research object, determined by the analytical method and the finite element method (FEM), does not exceed 10 %, and for the first three frequencies of the spectrum, it is no more than 6 %. Therefore, all methods are applicable. However, the use of an analytical expression allows calculations to be performed 40 times faster and does not require specialized software, making it more advantageous in frequency characteristics based design.
- 2. When calculating the natural frequencies using the finite element method, the second method of setting soil conditions allows a 5–6 times reduction in data entry time while yielding practically identical results.
- 3. Based on the analysis conducted for maximum productivity, it is recommended to use analytical expression (15) presented in this work when designing large-diameter pipeline transport structures.

Financing

This research was funded as part of a government assignment for the project: "Computer modeling of mechanical, thermal, and dynamic processes in weak and permafrost soils to ensure the reliability of ground foundations for engineering structures" (No. FEWN-2024-0006).

References

Alshabatat, N. and Zannon, M. (2021). Natural frequencies analysis of functionally graded circular cylindrical shells. *Applied and Computational Mechanics*, Vol. 15, No. 2, pp. 105–122. DOI: 10.24132/acm.2021.654.

Baghlani, A., Khayat, M., and Dehghan, S. M. (2020). Free vibration analysis of FGM cylindrical shells surrounded by Pasternak elastic foundation in thermal environment considering fluid-structure interaction. *Applied Mathematical Modelling*, Vol. 78, pp. 550–575. DOI: 10.1016/j.apm.2019.10.023.

Bochkarev, S. A. (2022). Natural vibrations of a cylindrical shell with fluid partly resting on a two-parameter elastic foundation. *International Journal of Structural Stability and Dynamics*, Vol. 22, No. 06, 2250071. DOI: 10.1142/S0219455422500717.

Dashevskij, M. A., Mitroshin, V. A., Mondrus, V. L., and Sizov, D. K. (2021). Impact of metro induced ground-borne vibration on urban development. *Magazine of Civil Engineering*, Issue 6 (106), 10602. DOI: 10.34910/MCE.106.2.

Dyachenko, I. A. Mironov, A. A., and Sverdlik, Yu. M. (2019). Comparative analysis of theories and finite element models for calculating free vibrations of cylindrical shells. *Transport Systems*, Issue 3 (13), pp. 55–63. DOI: 10.46960/62045_2019_3_55.

Ebrahimi, Z. (2022). Free vibration and stability analysis of a functionally graded cylindrical shell embedded in piezoelectric layers conveying fluid flow. *Journal of Vibration and Control*, Vol. 29, Issue 11–12, pp. 2515–2527. DOI: 10.1177/10775463221081184.

Farshidianfar, A. and Oliazadeh, P. (2012). Free vibration analysis of circular cylindrical shells: comparison of different shell theories. *International Journal of Mechanics and Applications*, No. 2 (5), pp. 74–80. DOI: 10.5923/i.mechanics.20120205.04.

Jain, A. K., Rawat, A., and Kushwah, S. S. (2016). Free vibration analysis of circular cylindrical shells. *American Journal of Engineering Research (AJER)*, Vol. 5, Issue 10, pp. 373–380.

Kumar, A., Das, S. L., and Wahi, P. (2015). Instabilities of thin circular cylindrical shells under radial loading. *International Journal of Mechanical Sciences*, Vol. 104, pp. 174–189. DOI: 10.1016/j.ijmecsci.2015.10.003.

Kumar, A., Das, S. L., and Wahi, P. (2017). Effect of radial loads on the natural frequencies of thin-walled circular cylindrical shells. *International Journal of Mechanical Sciences*, Vol. 122, pp. 37–52. DOI: 10.1016/j.ijmecsci.2016.12.024.

Lee, H. and Kwak, M. K. (2015). Free vibration analysis of a circular cylindrical shell using the Rayleigh–Ritz method and comparison of different shell theories. *Journal of Sound and Vibration*, Vol. 353, pp. 344–377. DOI: 10.1016/j. jsv.2015.05.028.

Leontiev, Y. V. and Travush, V. I. (2022). Fluctuations of pipelines of gas-containing liquids under changing bearing conditions. *Structural Mechanics of Engineering Constructions and Buildings*, Vol. 18, No. 6, pp. 544–551. DOI: 10.22363/1815-5235-2022-18-6-544-551.

Oliazadeh, P., Farshidianfar, M. H., and Farshidianfar, A. (2013). Exact analysis of resonance frequency and mode shapes of isotropic and laminated composite cylindrical shells. Part I: Analytical studies. *Journal of Mechanical Science and Technology*, Vol. 27, Issue 12, pp. 3635–3643. DOI: 10.1007/s12206-013-0905-1.

Piacsek, A. A. and Harris, N. (2019). Resonance frequencies of a spherical aluminum shell subject to prestress from internal fluid pressure. *The Journal of the Acoustical Society of America*, Vol. 145, Issue 3 (Suppl.), 1881. DOI: 10.1121/1.5101813.

Shahbaztabar, A., Izadi, A., Sadeghian, M., and Kazemi M. (2019). Free vibration analysis of FGM circular cylindrical shells resting on the Pasternak foundation and partially in contact with stationary fluid. *Applied Acoustics*, Vol. 153, pp. 87–101. DOI: 10.1016/j.apacoust.2019.04.012.

Shakiryanov, M. M. and Akhmedyanov, A. V. (2020). Nonlinear oscillations of a pipeline under the action of variable internal pressure and moving supports. *Journal of Machinery Manufacture and Reliability*, Vol. 49, Issue 7, pp. 555–561. DOI: 10.3103/S1052618820070134.

Shao, Y.-F., Fan, X., Shu, S., Ding, H., and Chen, L.-Q. (2022). Natural frequencies, critical velocity and equilibriums of fixed–fixed Timoshenko pipes conveying fluid. *Journal of Vibration Engineering & Technologies*, Vol. 10, Issue 5, pp. 1623–1635. DOI: 10.1007/s42417-022-00469-0.

Shui, B., Li, Y.-D., Luo, Y.-M., and Luo, F. (2023). Free vibration analysis of Timoshenko pipes conveying fluid with gravity and different boundary conditions. *Journal of Mechanics*, Vol. 39, pp. 367–384. DOI: 10.1093/jom/ufad031.

Sokolov, V. and Razov, I. (2020). Free oscillations of semi-underground trunk thin-wall oil pipelines of big diameter. In: Murgul, V. and Pasetti, M. (eds.). *International Scientific Conference. Energy Management of Municipal Facilities and Sustainable Energy Technologies. EMMFT-2018. Advances in Intelligent Systems and Computing*, Vol. 982. Cham: Springer, pp. 615–627. DOI: 10.1007/978-3-030-19756-8_58.

Tan, X. and Tang, Y.-Q. (2023). Free vibration analysis of Timoshenko pipes with fixed boundary conditions conveying high velocity fluid. *Heliyon*, Vol. 9, Issue 4, e14716. DOI: 10.1016/j.heliyon.2023.e14716.

Xü, W.-H., Xie, W.-D., Gao, X.-F., and Ma, Y.-X. (2018). Study on vortex-induced vibrations (VIV) of free spanning pipeline considering pipe-soil interaction boundary conditions. *Journal of Ship Mechanics*, Vol. 22, Issue 4, pp. 446–453. DOI: 10.3969/j.issn.1007-7294.2018.04.007.

Yulmukhametov, A. A., Shakiryanov, M. M., and Utyashev, I. M. (2020). Bending vibrations of the pipeline under the influence of the internal added mass. In: *AIP Conference Proceedings. Proceedings of the XXVII Conference on High-Energy Processes in Condensed Matter, dedicated to the 90th anniversary of the birth of RI Soloukhin, 29 June – 3 July 2020, Novosibirsk, Russia, Vol. 2288, Issue 1, 030093. DOI: 10.1063/5.0028885.*

СОБСТВЕННЫЕ КОЛЕБАНИЯ СТАЛЕБЕТОННОЙ ЦИЛИНДРИЧЕСКОЙ ОБОЛОЧКИ В ГРУНТОВОЙ СРЕДЕ

Андрей Викторович Дмитриев* (Andrei Dmitriev), Владимир Григорьевич Соколов (Vladimir Sokolov), Татьяна Владимировна Мальцева (Tatyana Maltseva)

Тюменский индустриальный университет, ул. Володарского, 38, Тюмень, Россия

*Email: dmitrievav@tyuiu.ru

Аннотация

Введение. Цилиндрические оболочки, уложенные в грунтовую среду, как правило, используются в трубопроводном транспорте. Для исключения повреждения трубопроводов бетонными утяжелителями при всплытии конструкции в обводнённой среде, предлагается использовать трубобетонные изделия, внутренняя часть которых выполняется из стали, а внешняя часть образована бетонным слоем толщиной 30-50 мм. Перед проектировщиком в таком случае становится вопрос, какой из методов расчёта использовать для нахождения частот собственных колебаний. Цель исследования: Сравнить значения частот собственных колебаний сталебетонного газопровода большого диаметра в грунте, полученные при помощи аналитической зависимости со значениями, определёнными в программном комплексе ПК Lira. **Методы:** Первый метод определения частоты основывается на использовании аналитического выражения, которое было получено с использованием полубезмоментной теории цилиндрических оболочек. Второй базируется на методе конечных элементов с построением расчётной модели в среде Lira Sapr. Моделирование в программном комплексе слоёв стали и бетона композитной оболочки осуществлялось 4-х узловыми пластинами, которые объединены в общую структуру при помощи абсолютно жёстких тел (АЖТ). Учёт грунтовой среды, окружающей оболочку, в первом случае выполнялся путём создания массива (размером 5,3×5,3 метров) объемными телами, во втором случае путём задания коэффициента пастели для бетонного слоя. Результаты: Установлено, что второй способ задания грунтовых условий позволяет сократить время ввода данных в 5-6 раз при одинаковых результатах. Расхождение частот собственных колебаний для объекта исследования, определённых аналитическим методом и МКЭ не превышает 10 %, а для первых 3-х частот спектра не более 6 %, следовательно, все методы применимы. Однако использование аналитического выражения позволяет вычислять результаты в 10 раз быстрее и не требует специализированного программного обеспечения, поэтому является более выгодным при отстройке конструкции по частотным характеристикам.

Ключевые слова: собственные колебания; метод конечных элементов; полубезмоментная теория цилиндрических оболочек; частота.